

Review

Review of Nanoscale Vacuum Devices

Xinghui Li and Jinjun Feng * 

National Key Laboratory of Science and Technology on Vacuum Electronics, Beijing Vacuum Electronics Research Institute, Beijing 100015, China

* Correspondence: fengjinjun@tsinghua.org.cn

Abstract: The newly developed nanoscale vacuum devices have basic functions similar to traditional vacuum tubes, but can be manufactured by existing silicon-based process lines to achieve small size, light weight, and high integration, which makes them attractive, especially in the recent decade. The historic development and the state-of-the-art of the nanoscale vacuum devices are reviewed. It is found that the devices with lateral, vertical, and gate-all-around structures all have their own advantages and drawbacks. Silicon has the most mature process, but the silicon nanoscale vacuum devices show poor electrical properties and low endurance to harsh conditions when compared with their metal or wide bandgap semiconductor competitors. Even though the most developed nanoscale vacuum devices today still cannot cope with the solid-state devices or integrated circuits (ICs) in most normal applications, they are expected to be first employed in environments with high temperatures or strong radiation.

Keywords: nanoscale vacuum device; structure; material; temperature resistance; radiation endurance

1. Introduction

Since their invention in the 1900s, vacuum tubes have experienced vigorous development and dominated the areas of electrical signal amplification, switch, or modulation for decades. However, the large, fragile, and inefficient devices with high vacuum sealing and high-temperature thermionic electron sources were replaced gradually by solid-state semiconductor transistors and diodes as well as the consequent integrating circuits in almost all applications [1], with the exception of hi-fi sound systems [2], high-power systems and radio base stations [3,4], and high-frequency microwave and terahertz devices [5,6].

The traditional vacuum tubes can still rival solid-state mainly because the carriers' (for the former, mainly electrons; for the latter, electrons and holes) transport medium is a vacuum. Compared with semiconductors, a vacuum offers unique and unsurpassed characteristics; therefore, the vacuum tubes have some obvious advantages: a vacuum allows electrons' ballistic transport without optical and acoustic phonon scattering, so the devices have minimal signal distortion; the electrons in a vacuum can be accelerated to a very high speed close to light speed, so the devices have fast conversion speed; the electrons in a vacuum can work under very high voltage and current conditions, so the devices can output high power. Moreover, the vacuum tubes are intrinsically superior to the semiconductor devices in harsh environments with respect to temperature and radiation. The radiation resistance of vacuum tubes is because vacuum has no radiation-induced defects in solid semiconductors, and it also cannot be directly damaged by particle bombardment, which is urgently required in some important application scenes, for example, spacecrafts [7].

The fact that semiconductors defeat vacuum tubes in many areas is not due to material superiority nor to device performance, but to the ease of batching the microfabrication process and, consequently, the miniaturization, lightness, low-cost, low-power consumption, and integration performance of the devices. In other words, traditional vacuum tubes with principle advantages are seriously hindered by their awkward processing methods. Naturally, a simple idea is to make vacuum tubes by the microfabrication technology



Citation: Li, X.; Feng, J. Review of Nanoscale Vacuum Devices. *Electronics* **2023**, *12*, 802. <https://doi.org/10.3390/electronics12040802>

Academic Editor: Alessandro Gabrielli

Received: 3 January 2023

Revised: 25 January 2023

Accepted: 31 January 2023

Published: 6 February 2023



Copyright: © 2023 by the authors. Licensee MDPI, Basel, Switzerland. This article is an open access article distributed under the terms and conditions of the Creative Commons Attribution (CC BY) license (<https://creativecommons.org/licenses/by/4.0/>).

developed for on-chip large-scale integration of micron-sized solid-state devices; therefore, the new fabricated micro-vacuum-tubes can combine both advantages of vacuum and solid-state devices. In fact, in the early 1960s, before modern microfabrication technology came into existence, K R Shoulders proposed vacuum tunnel effect devices of micron sizes and realized them with advanced machining techniques [8].

Shoulders' proposal encountered great difficulties for a very long time because of two reasons: one is the mechanical processing and manual assembly modes which are more applicable to discrete devices, and the other is the commonly used high-temperature thermionic cathodes which are hard to miniaturize or integrate. In fact, the thermionic cathode, mechanical processing, and manual assembly are still the mainstream configurations for most discrete vacuum devices today, except for some high-frequency terahertz power devices whose slow-wave structures really need modern microfabrication technologies such as LIGA or DRIE. The emergence and gradual improvement of the Spindt cathode in the 1960s–1970s made the devices come true [9,10]. The metal tip field emission cold cathode and its microfabrication technologies can overcome the above two obstacles simultaneously. In 1986, H F Gray showed the fabrication of a vacuum field effect transistor and vacuum integrated circuit based on a silicon tip field emission cathode, which was a fine example of the use of state-of-the-art silicon fabrication technology in building vacuum devices at that time [11]. C A Spindt and H F Gray's efforts gave birth to the so-called vacuum microelectronic devices. However, the micron-sized vacuum devices still need dozens to hundreds of volts to induce field emission, and so they also need high vacuum sealing used for traditional vacuum devices to avoid fatal discharge. Therefore, it is difficult for those kinds of vacuum microelectronic devices to achieve high performance with high reliability.

Reducing the electrode distance and decreasing the operation voltage are critical factors for the miniaturization and high reliability of vacuum devices, which heavily depend on the advanced microfabrication ability. It is difficult for the 1990s' common planar microfabrication technologies to realize a lateral field emission transistor well with an electrode distance below 1 μm [12], and an over-closed gate to the cathode can lead to electron capture for that lateral structure. In 1997, A A G Driskill-Smith presented a vertical field emission device. By controlling the thickness of the insulator film rather than the lithography critical dimension, the distance between the emitter and the gate was reduced to tens of nanometers [13]. Consequently, the device has a turn-on voltage as low as 7.5 V and it can work stably in atmosphere for a long time. However, the device does not attract much attention because of an obvious shortcoming: the emitters in the vertical cavity are formatted by a random process, which makes it very difficult to achieve highly identical geometrical dimensions of the devices on one substrate.

The rapid development of microfabrication technology reduced the critical dimensions to real nanoscale, which promoted the appearance of nano vacuum devices. In 2012, J W Han et al. proposed a nanoscale vacuum channel transistor [14], and S Srisonphan et al. proposed a vacuum channel metal oxide semiconductor (MOS) field effect transistor [15]. Although, with quite different names and structures, the two devices have two revolutionary common features: one is that the electrode gaps of the devices are all in nanometer scale, which are less than or near to the mean free path of electrons in air; the other is the operating voltages of the devices are all below 10 V, which keeps the electrons' energy less than the air molecules' first ionization energy in the whole working process. The features ensure the devices achieving ballistic electron transmission even in atmosphere without the risk of air discharge. For simplicity, these kinds of devices are uniformly called nanoscale vacuum devices next.

The nanoscale vacuum devices based on the most advanced microfabrication technology broke through the traditional vacuum electron device mode and attracted wide attention at that time. Some researchers believe that the devices may replace the existing MOS transistors to achieve high-speed switching and signal amplification, and the vacuum-integrated circuits could also compete strongly with solid-state integrated circuits [16–18].

Many research institutions have begun to pay attention to the devices and technologies, and have followed up to study the device principles, materials, and processes. In this article, an up-to-date review of nanoscale vacuum devices is presented. Here, the devices refer to nanoscale vacuum diodes, vacuum triodes (called vacuum transistors in some of the literature), and some field emission cathodes. Because the field emission electron sources are the basic elements of the vacuum devices, some of them, for example, the Spindt cathodes, can be directly used as vacuum diodes. The structures and materials of the devices are mainly involved, and future applications are considered.

2. Structures

According to the related locations of emitter, gate, and collector (or cathode, gate, and anode for a so-called triode; or source, gate, and drain for a so-called transistor), the nanoscale vacuum devices are generally categorized into horizontal, vertical, and gate-all-around (GAA) structures [19].

2.1. Lateral Structures

The horizontal structure was also named as a lateral structure in the literature. One simple lateral nanoscale vacuum device has coplanar electrodes, thus all the electrodes of the device, usually including a cathode, an anode, and a pair of gates, can be formed by one patterning process, which is compatible with microfabrication technology.

The coplanar diodes with nanogaps are commonly used as rectifiers, switches, or test samples for electron emission performance study. T Higuchi et al. proposed and demonstrate a two-nanotip-based nanoscale vacuum diode triggered by few-cycle near-infrared laser pulses. The laser-triggered current between a sharp-blunt tip pair exhibits a rectifying behavior, which is in analogy to classical vacuum-tube diodes. Although the gap width exceeds 100 nm, the total operation time of this laser-triggered nanoscale diode is estimated to be below 1 ps [20].

W M Jones et al. demonstrated a novel fabrication technique using silicon on insulator substrates to reliably produce sub-20 nanometer gaps between deposited emitter and collector metals in symmetric two-terminal field emission devices. The emitters demonstrate repeatable, low voltage emission across a range of metals. The device can operate at room temperature atmospheric pressures and at temperatures as high as of 215 °C in vacuum atmosphere [21].

W T Chang et al. fabricated field emission diodes with metal-based asymmetric electrodes by electron beam lithography, as shown in Figure 1. The cathode is made up of multiple triangles and the anode is made up of multiple semicircles. This kind of design can effectively enhance the forward/reverse current ratio, suggesting that asymmetric cathode and anode design can serve as an FE diode. The minimal anode-cathode distance of the device is approximately 24 nm, and the field emission occurred at a potential less than 0.5 V [22]. The group then proposed a voltage adder formed by two field emission air-channel (FEAC) devices. The cathode and anode of the device are eight-pair tip-to-tip patterns fabricated by electron beam lithography, as shown in Figure 2. The voltage adder can work at less than 1 V with an approximately 40 nm anode-cathode gap [23].

M Liu et al. fabricated nanogaps with an emitter-to-collector distance of 10 nm with the aid of focused ion beam etching. Due to the extremely small electrode gap, high emission currents and excellent emission stability were achieved in air with a turn-on voltage as low as 0.46 V [24]. K R Sapkota et al. demonstrated a vacuum nanodiode consisting of a wedge-shaped emitter and a flat rectangular collector by using electron-beam lithography and a two-step top-down dry plus wet etch process. For a diode with a sharper emitter tip of 17 nm radius and a gap size of 30 nm, an ultralow turn-on voltage of 0.24 V and nearly 0.5 μ A current at only 1 V are achieved in air at atmospheric pressure [25].

The design idea of a nanoscale vacuum triode comes from its microscale predecessors [12,26,27]. By using the top photolithography and LOCOS technology in 1999, Lee et al. fabricated a lateral field emission triode with an anode-to-cathode distance of 6.5 μ m, a gate-to-emitter distance of 1 μ m, and a gate aperture of 1.5 μ m; the schematic diagram of it

is shown in Figure 3. Although all the critical dimensions are far more than the nanometer scale, the turn-on voltage of it reduces to as low as 14 V [12]. Afterwards, in 2001, L L Pescini et al. reduced the critical dimensions of a device with the same structure by using electron beam lithography. The fabricated lateral field-emission triode has a cathode-to-gate distance of 150 nm. The triode exhibits a very low turn-on voltage of about 1.5 V with a current level of 4 nA; it can continuously work from high vacuum to atmosphere for several weeks without severe degradation effects [28].

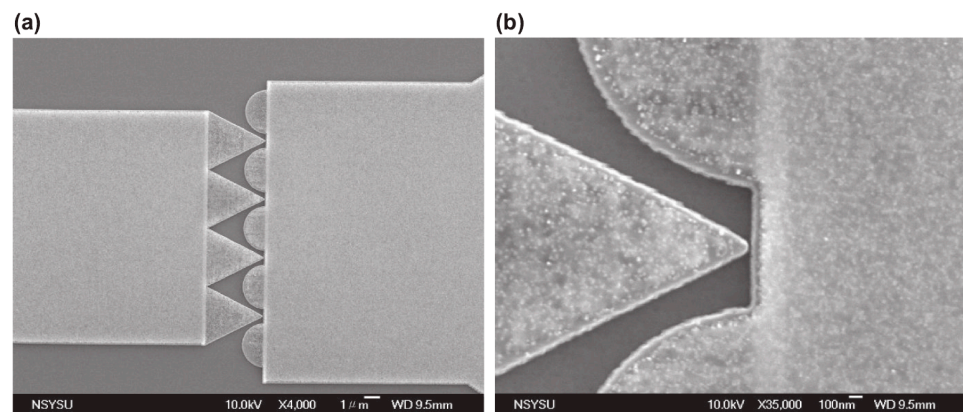


Figure 1. (a) Field emission diode comprising four triangles on one side and five semicircles on the opposite side. (b) Minimal distance of approximately 24 nm between the terminals of the two electrodes located between the triangular apex and the flat side [22].

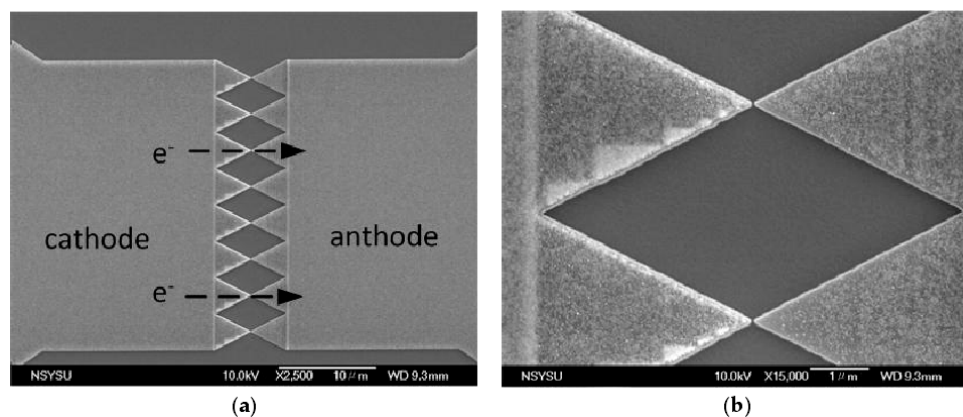


Figure 2. (a) Micrograph of an eight-pair tip-to-tip pattern as a field emission air channel, (b) the tip-to-tip gaps are approximately 40 nm [23].

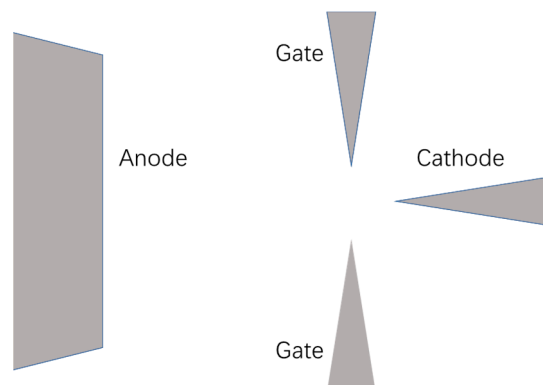


Figure 3. Schematic diagram of a microscale lateral field emission triode.

Through the precise control of electron-beam lithography, the critical dimensions of the device can be fine-tuned on a nanometer scale. W T Chang et al. fabricated the coplanar structures with a tip-to-tip distance as low as 35 nm, as shown in Figure 4, and systematically investigated the effects of the gate pair on the electron emission performance. The result indicated that for a nanoscale cathode-to-collector distance, the gate pair in the perpendicular direction with increasing potential can attract and intercept a portion of electron emission, which eventually lowered the electric field on the emission surface and reduced the collector current. Although the electron extracting function is greatly weakened, the gate pair can disrupt electron emission and eventually turn on/off the current, which allows the device to achieve logic application [29]. The coplanar gate pair and their roles in nanoscale channels became major issues due to electron interception; the result was consistent with the conclusion made by J Kim et al. [30].

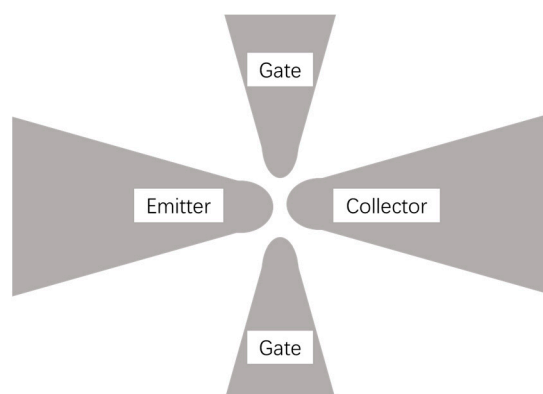


Figure 4. Schematic diagram of a coplanar field emission device with an emitter-collector distance of 35 nm.

To reduce the gate leakage of the coplanar vacuum triode, J W Han proposed a gate insulated nanoscale vacuum channel transistor based on the structure of a metal-oxide-semiconductor field-effect transistor (MOSFET) [14,31], in which the emitter (source) and the collector (drain) are coplanar, and the gate is insulated from them below by a thin oxide layer. The emitter-to-gate distance is determined by the very thin insulator film, which is sharply pointed to intensify the electric field at the emitter tip, as shown in Figure 5. Through 0.18 μm optical lithography and photoresist trimming technology, an emitter-to-collector distance down to 150 nm is achieved. The working voltage of the device is less than 10 V and the cut-off frequency is 0.46 THz. Han's device is totally obtained by a silicon fabrication process; it is co-fabricated easily with a mature MOSFET on a silicon-on-insulator wafer and shows a turn-on voltage of 2 V at a cell current of 2 nA and a cell current of 3 μA at the operation voltage of 10 V with an on/off current ratio of 10^4 [32]. To obtain an emitter-to-collector distance less than 100 nm, microfabrication technologies other than optical lithography must be used.

J Xu et al. demonstrated aligned sub-30 nm vacuum nanogap arrays by using electron beam lithography and focused ion beam technology. With the new approaches, it is possible to integrate vacuum transistors in the scale as little as 10 nm and, therefore, enable a new generation of high-performance, high-speed, and low-cost electronic devices [33]. S Nirantar et al. presented nano-scale metal-based field emission air channel transistors. With electron beam lithography, symmetric and sharp source and drain electrodes are achieved with tip-to-tip distances from 11.5 nm to 34.1 nm, as shown in Figure 6. The devices operate in a bi-direction with voltages less than 2 V and current values in the range of a few tens of nA [34].

2.2. Vertical Structures

Initial vertical vacuum diodes and triodes are mostly based on a sharp tip with a very near self-aligned round gate, for example, the Spindt type cathodes as shown in Figures 7

and 8 [35,36], because this structure is capable of achieving the strong electric field required for electron emission with an appropriate gate voltage. C O Bozler et al. first scaled the Spindt cathode down to nanometer range. By using laser interferometric lithography, gate holes with a diameter of 160 nm were obtained and the tip-to-gate spacing was only 80 nm. The nanoscale Spindt cathode showed a low turn-on voltage of 8 V and a record emission current density of 1600 A/cm² for that structure [37].

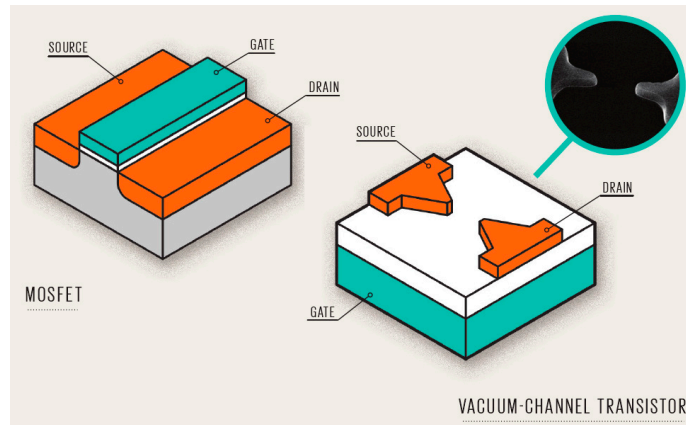


Figure 5. The structural analogy between the back-gate MOSFET and the back-gate nano vacuum-channel transistor [31].

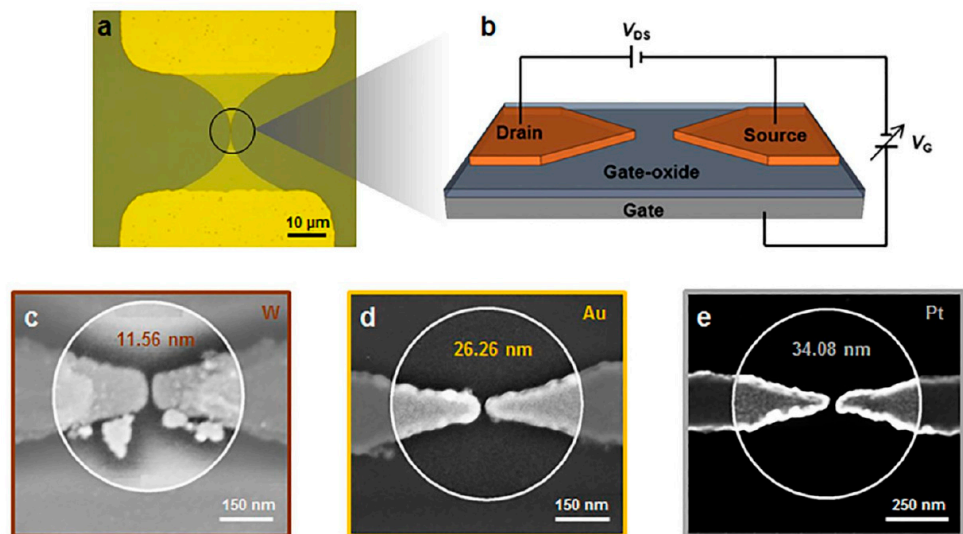


Figure 6. (a,b) Metal-air transistor structure and (c–e) high-resolution images of nano-gap metal electrode [34].

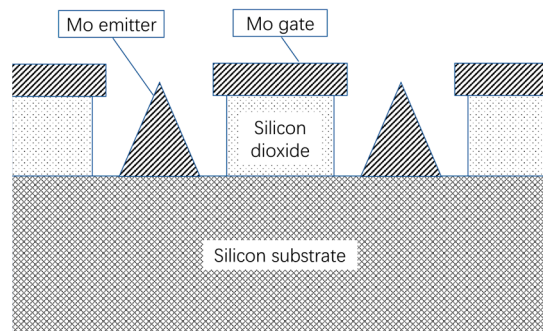


Figure 7. Schematic diagram of a Spindt cathode.

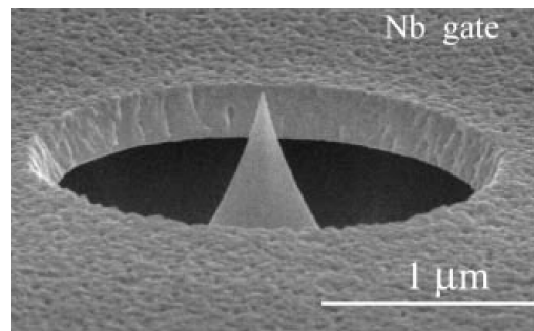


Figure 8. SEM photo of a Si-tip Spindt-type cathode [36].

It is difficult to achieve the vertical tip of gate structures with highly identical geometrical dimensions on one substrate. H K Kim et al. proposed a vacuum nanochannel transistor based on film edge emission. The device is fabricated by etching square holes into stacked films consisting of metal, oxide, and a semiconductor using focused ion beam technology. The exposed film edges inside the holes are used as electrodes. For a two-terminal device, the stacked films are metal and oxide on a silicon substrate; while for a three-terminal device, the stacked films, in turn, are metal, oxide, conductive indium-tin oxide (ITO), and oxide on a silicon substrate, as shown in Figure 9. The channel length between electrodes of this vertical structure is determined precisely by the thickness of the oxide layer and is easily defined to about 20 nm. The turn-on voltage of the devices is about 0.5 V, the two-terminal device demonstrates a rectifying behavior with an on/off ratio of 500, and the three-terminal device demonstrates a clear, well-defined field-effect transistor (FET) characteristic at atmosphere [15].

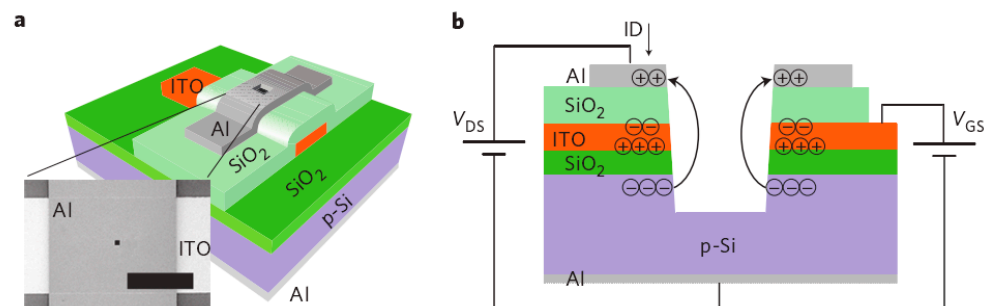


Figure 9. Schematic diagram of a nano-void channel field emission transistor: (a) titled view and (b) cross-sectional view [15].

In order to make Kim's device more compatible with digital integrated circuits, I J Park et al. proposed to greatly decrease the anode voltage and the ratio of the gate-to-cathode distance to the channel length under the condition of keeping the channel length less than the mean free path of electrons in air. A slit-type vacuum-channel transistor with a gate-to-cathode distance of 2 nm and a gate-to-anode distance of 30 nm was designed, and the simulation result indicates that there is not any gate leakage current when the gate bias is the same as the anode bias [38].

S L Wu et al. proposed a device structure similar to Kim's, but with a cylindrical vacuum channel other than a square one. Accordingly, the cathode and gate of this transistor possess an annular ring structure, and the electric field on the emission surface and the density of electrons concentrated near the cathode edge are uniform. This characteristic may effectively reduce device failure resulting from extremely intense local electrical fields. The simulation of the device shows that the threshold voltage varies from 1.2 V to 3.3 V for dielectric thickness from 10 nm to 20 nm, and the vacuum channel radius should be no less than 20 nm to avoid severe performance degradation due to the gate shield effect [39]. W T Chang et al. investigated the effect of different gate locations (3 nm, 10 nm, 20 nm,

and 30 nm away from the cathode, respectively) in the stack-film vertical field emission air-channel transistor with a fixed cathode-to-anode distance near to the electron mean free path in air [19]. The particle trajectory model indicates that the transistor with a short emitter-to-gate distance exhibits better control on electron emission, and the behavior of the I-V plot is similar to typical MOSFETs, which is consistent with the research of I J Park and S L Wu. Reducing the gate oxide thickness alone brings two problems, one is the increased gate-to-source capacitance, which is unfavorable to the improvement of transconductance, and the other is the increased risk of emitter-gate leakage.

J W Han et al., therefore, proposed an extended gate structure, in which the gate is folded near the emitter edge region, so that the gate oxide in the field region is thick, whereas near the emitter edge it is thin, as shown in Figure 10. By introducing dual oxide structures with different thickness values, the nanoscale vacuum channel transistor with extended gate decouples the gate-to-emitter capacitance and the gate-to-emitter overlap capacitance and can achieve both low parasitic capacitance and low current leakage simultaneously [40].

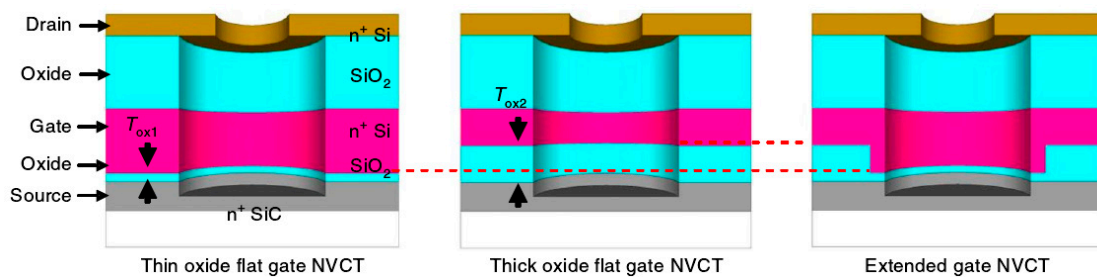


Figure 10. Schematic illustration of thin oxide nanoscale vacuum channel transistor with folded gate [40].

2.3. Gate-All-around Structures

As the name suggests, the gate-all-around (GAA) device features the gate and the gate insulator fully surrounding the active channel body and thus providing the best possible electrostatic control [41]. The GAA structures can be further categorized into vertical and lateral structures. In fact, the aforementioned vertical gated tip structures, for example the Spindt-type cathodes, are typical vertical GAA structures. These kinds of structures played important roles in vacuum microelectronic devices but almost disappeared in nanoscale vacuum devices. The reason is exactly as the one explained in Section 2.2, which is more obvious in nanoscale devices.

The lateral gate-all-around structure was first used in a MOS device [42]. Mature techniques (top-down and bottom-up) were established for the fabrication of lateral GAA MOSFETs [43], and on this basis, a FET with vacuum gate dielectric was proposed and achieved by adding a sacrificial layer deposition and removal process [44,45], as shown in Figure 11.

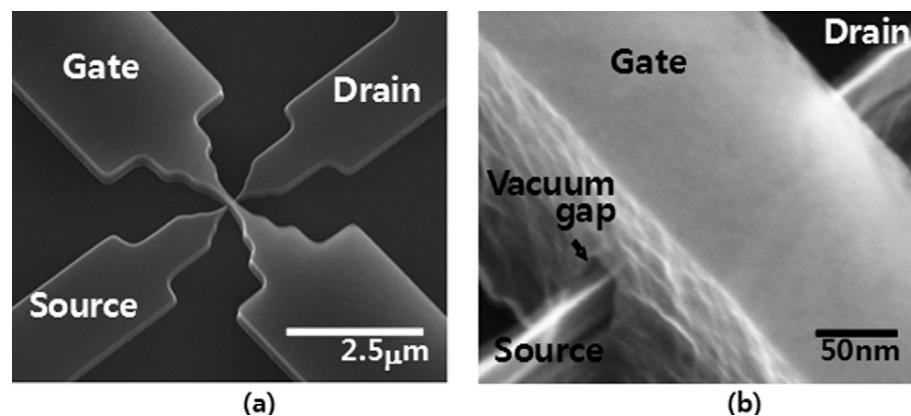


Figure 11. SEM images of vacuum gate dielectric gate-all-around field effect transistor: (a) bird's-eye view and (b) magnified view of the vacuum gap region [45].

Considering the outstanding performance of GAA structures in conventional Si nanoscale devices, a lateral GAA vacuum field-effect transistor (VFET) was proposed by J Kim et al. Due to excellent gate controllability, the GAA VFET with short channel length and thin channel-to-gate distance would be most suitable for low power consumption and less sensitivity to device fluctuation. The simulation results indicate that the GAA VFET can work at a lower voltage helping to circumvent the high-power issues of vacuum electronics when compared to single- and double-gate structures [30].

By replacing the nanowire of the device in [45] with a vacuum channel, J W Han et al. fabricated a lateral GAA VFET. The transistor consists of sharp source and drain electrodes separated by a sub-50 nm vacuum channel with a source-to-gate distance of 10 nm, and it operates at a voltage less than 5 V providing a high drive current of above 3 μA [46].

2.4. Other Structures

A new structure also based on stacked films consisting of metal, oxide, and a semiconductor was proposed recently. Instead of etching down holes in stacked films, the new devices use stacked film pads on the substrate as the electrode structures. By using an IC-compatible process including chemical vapor deposition, lithography, and chemical etching, two diode structures capable of achieving high emission currents were carried out. M Liu et al. [47] and M Li et al. [48] fabricated a SiO_2 insulator and a gold pad on silicon and GaN substrates, respectively; the schematic diagram of the latter is shown in Figure 12. Emission currents from several hundred microamperes to milliampere levels can be obtained from one single pad structure of the devices. The high currents are mainly due to the long emission edges of the pad or the large emission areas around the pad edge.

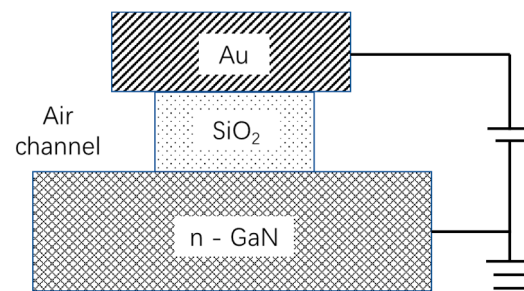


Figure 12. Schematic diagram of a nanoscale air channel device.

Similar to this design concept, J W Han et al. [49] proposed a gated diode (in fact a three-terminal structure), in which pads of an anode insulator, anode, cathode insulator, and an umbrella-shaped cathode are fabricated in turn on a silicon substrate, as shown in Figure 13. Unlike in the traditional transistors with the gate typically located between the source and the drain, the bottom silicon substrate becomes the gate and the anode terminal is located between the umbrella cathode and the gate. The fabricated devices show excellent diode characteristics and the gated diode structure is attractive for extremely low gate leakage.

In summary, the nanoscale vacuum devices mainly have lateral structures, vertical structures, and gate-all-around structures, and all of them have their strengths and weaknesses, as shown in Table 1. The lateral structures have the best compatibility with traditional IC technologies, but it is hard to achieve wafer-scale critical dimension uniformity without the most advanced DUV or EUV lithography equipment. The vertical structures can readily realize a precise air channel, but the high parasitic capacitance and current leakage between the cathode and the gate are the intrinsic disadvantages of this structure. Although some solutions are proposed, the new design still needs practical verification. The gate-all-around structures have the most effective control of the emission, but they have more complex structures and need a more difficult fabrication process when compared with the other two structures.

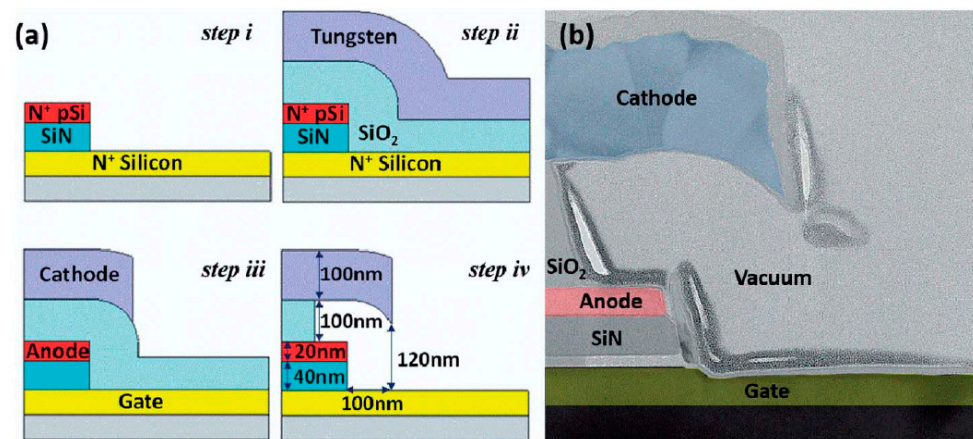


Figure 13. A vertical vacuum field emission gated diode with an umbrella cathode: (a) schematic illustration of the fabrication, (b) cross-sectional TEM image of the device [49].

Table 1. Strengths and weaknesses of nanoscale vacuum devices with different structures.

Device Structure	Strength	Weakness
Lateral structure	Good compatibility with ICs	Poor critical dimension Uniformity
Vertical structure	Precise air-channel control	High parasitic capacitance and current leakage
GAA structure	Effective control of emission	Complex structure and difficult fabrication

3. Materials

Materials are also key factors for the nanoscale vacuum devices; they influence not only the performance of the devices but also the resistance to operating conditions such as temperature, atmosphere, and radiation, etc. The materials of initial nanoscale vacuum devices come from their microscale predecessors. Silicon dominates traditional integrated circuits because of its good thermal stability, the oxide with dense and high dielectric constant, and the easy preparation of a silicon–silicon oxide interface with few interface defects. It also plays important roles in nanoscale vacuum electronic devices. In the pioneering devices of J W Han and S Srisonphan, silicon is used both as the substrate and the electrode. And in many follow-up nanoscale vacuum devices, silicon material and silicon technology still occupy important positions.

However, the easy oxidation and the poor field emission ability of silicon limit the improvement of device performance. Other materials after silicon are used in nanoscale vacuum devices; aluminum is adopted mainly because of its excellent processing compatibility with traditional IC, gold and platinum are used because of their good chemical stabilities, and refractory metals such as molybdenum and tungsten are used because of their good field emission performance. Moreover, some new materials are also attempted in the devices gradually.

C Lenk et al. carried out an experimental study of field emission from ultrasharp silicon, diamond, GaN, and tungsten tips in close proximity to the counter electrode, and the result indicated that the emission process follows the Fowler–Nordheim dependency for metals or semiconductors, for which the electron emission occurs mainly from the valence band [50].

3.1. Metals

S Nirantar et al. investigated the electron emission performance of different metals used as source and drain electrodes with a planar, symmetric, and sharp geometry with an air channel length of less than 35 nm. The experimental data show that the influential operation mechanism is Fowler–Nordheim tunneling in tungsten and gold devices, while Schottky emission in platinum devices [34]. R. Bhattacharya et al. carried out long-

term field emission current stability characterization of planar field emitter devices with gold/titanium electrodes. The nanoscale devices have 10–20 nm tip-to-tip or tip-to-collector dimensions; when placed on lifetime tests in a vacuum of $<10^{-8}$ Torr and biased at 6 V DC, nearly half of the tested devices show $<5\%$ degradation in current until 1400 h when testing is stopped, indicating good long-term working performance [51].

X Li et al. investigated the environment adaptability and analyzed failure reasons of a nanoscale vacuum channel transistor with a vertical structure. The molybdenum-emitter-based device has basically unchanged I-V performance in a wide vacuum range from 10^{-7} Pa to 10^4 Pa. Although the ordinary operating current of the device is only tens of nanoamperes with a voltage less than 10 V, it can work under the strong electric field under a bias voltage of 50 V, and meanwhile, can endure the Joule heating resulting from several microampere emission currents and an annealing treatment temperature up to $400\text{ }^{\circ}\text{C}$ [52].

L B De Rose et al. presented suspended lateral two-terminal diode-like and four-terminal triode-like vacuum field emitters for high-temperature operation. Tungsten film is patterned on a silicon nitride membrane as an emitter due to its low work function and high-temperature tolerance, and the insulator in the vicinity of the terminals is removed to increase the resistance of leakage current pathways. The two-terminal device is tested for temperatures ranging from $150\text{ }^{\circ}\text{C}$ to $450\text{ }^{\circ}\text{C}$, and the four-terminal device can work normally up to $300\text{ }^{\circ}\text{C}$ [53].

3.2. Graphene

The appearance of graphene gave birth to an entirely new research branch of solid-state electronics [54]. Graphene is a one-atom-thick allotrope of carbon, with unusual two-dimensional Dirac-like electronic excitations. Through proper deformation and combination, graphene can become graphite, carbon nanotubes, and fullerenes, as shown in Figure 14 [55,56]. Due to their metallic character and two-dimensional (2D) nature, heterojunction transistors with graphene-controlling elements can potentially achieve high operation frequencies and show unconventional or improved performances compared to traditional semiconductor transistors [57,58].

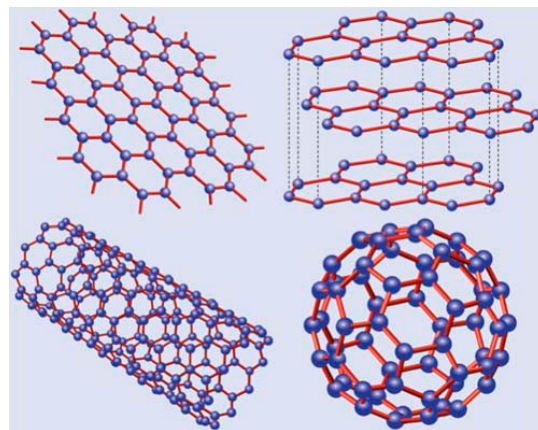


Figure 14. Schematic diagram of graphene (**top left**), graphite (**top right**), carbon nanotube (**bottom left**), and fullerenes (**bottom right**).

X Wei et al. proposed a vertical graphene vacuum transistor (GVT), employing electrically biased graphene as the electron emitter. The states of the device are switched by tuning the bias voltage (<10 V) applied to the graphene emitter with an ON/OFF current ratio up to 10^6 , exhibiting a switching performance superior to those of reported graphene-based solid-state transistors. A symmetric ambipolar device is achieved by GVT integration and has the potential of realizing vacuum-integrated circuits based on GVTs, which are expected to be applied in extreme environments such as high temperature and intense irradiation [59].

J Xu et al. reported the fabrication and electrical performance of a lateral nanoscale vacuum channel transistor (NVCT) based on graphene electrodes. An emitter-to-collector distance of 90 nm is achieved by using electron beam lithography. The gated device exhibits an on/off current ratio of up to 10^2 with a low working voltage of less than 20 V and a small leakage current of less than 0.5 nA and represents a promising candidate for high-speed applications [60].

Although with excellent overall performance, graphene usually needs to be transferred onto the process wafer rather than direct growing, which hinders its batching fabrication.

3.3. Silicon Carbide

Due to the elimination of p-n junctions, the maximum operating temperature for silicon MOSFETs is limited to approximately 300 °C, while a silicon carbide (SiC) transistor can work to 600 °C [61], and SiC nanoneedle field emitting arrays can be operated at 500 °C [62].

SiC is a robust material with appealing work function (n-type 4H-SiC: ~4 eV; Si: 4.6 eV) and established fabrication processes. One-dimensional SiC nanostructures can be an ideal candidate for field emitters owing to their superior properties such as a large bandgap (4H-SiC: 3.26 eV; Si: 1.1 eV), outstanding mechanical properties, excellent chemical inertness, good thermal conductivity (4H-SiC: 4.7 W/cm·K; Si: 1.5 W/cm·K), and high thermal stability. M Liu et al. fabricated individual SiC emitters with a nanogap from single crystal silicon carbide nanowire with the help of FIB etching. The controlled etching allows systematic variation of the anode-cathode distance from 20 to 120 nm. Field electron emission is turned on at 3.2 V for an electrode gap of 20 nm and a current of 22.3 nA is achieved at 5 V. The results for the diode-based system are useful for the design of gated three-terminal devices, for example, vacuum field emission transistors [63].

J W Han et al. fabricated their nanoscale vacuum channel transistors with extended gate structures on SiC wafers. The SiC vacuum channel transistors offer superior long-term stability when compared to identically sized silicon ones. Moreover, the devices also offer a robustness against total dose radiation and displacement damage. In the total ionizing dose effect test by using a Co-60 source, no significant performance degradation for a total dose of up to 30 krad is found, which corresponds to approximately 10 years at an altitude of 800 km. Additionally, the displacement damage test by fast neutron irradiating shows that no degradation is observed for a peak neutron energy of 10 MeV at a fluence of $\sim 1 \times 10^{14}$ ncm⁻² [40].

The large bandgap energy of SiC offers advantages over silicon in terms of high-temperature endurance. Since every spacecraft is required to go through a thermos-radiation sterilization process involving dry baking at around 600 °C under high-dose radiation, nanoscale vacuum transistors fabricated on silicon carbide wafers are expected to provide radiation-tolerant electronics for application in future spacecrafts because of the superior resistance characteristics against various types of radiation and high temperatures [7].

3.4. Gallium Nitride

The III-nitride semiconductors are attractive for their high thermal and chemical stability, low electron affinity, and high breakdown fields, and gallium nitride (GaN) was used as field emission material because of its good performance long before. Pyramidal array and line/rod array GaN emitters were realized by the elective area growth technique [64] and the three-dimensional epitaxial technique [65], respectively, and good field emission results were obtained.

GaN has many superior properties for field-emission vacuum nanoelectronics, including low electron affinity (can be negative), high electron mobility (GaN: 2000 cm²/v·s; Si: 1350 cm²/v·s), a large bandgap (GaN: 3.4 eV; Si: 1.1 eV), high thermal and chemical stability, and a high breakdown field (GaN: 3.3 kV/cm; Si: 0.3 kV/cm). Recently, employing GaN in nanoscale vacuum devices attracted more attention due to its radiation endurance in addition to its excellent field performance. GaN-based devices are more radiation hard than their Si and GaAs counterparts due to the high bond strength in III-nitride materials [66].

D S Zhao et al. reported an $\text{Al}_{0.25}\text{Ga}_{0.75}\text{N}/\text{GaN}$ -based lateral field emission device with a nanometer scale void channel of ~ 45 nm. Under atmospheric conditions, the GaN-based field emission device shows a low turn-on voltage of 2.3 V, a high emission current of ~ 40 μA at a collector bias of 3 V, and a low reverse leakage of 3 nA at -3 V. These characteristics are attributed to the nanometer scale void channel as well as the high density of two-dimensional electron gas in AlGaN/GaN heterojunction [67].

K R Sapkota et al. reported top-down fabricated, lateral gallium nitride (GaN)-based nanoscale vacuum electron diodes operable in air, with record ultra-low turn-on voltages down to ~ 0.24 V, and stable high field emission currents, tested up to several microamps for single-emitter devices. The device consists of only GaN, in which carbon-doped GaN is used as the insulator and Si-doped n-type GaN as the emitter and collector. It has high resistance to damage from 2.5 MeV proton exposure, which shows promise for a new class of high-performance and robust, on-chip, III-nitride-based vacuum nano-electronics operable in air or reduced vacuum with radiation [25,68].

M Li et al. introduced GaN in a nano diode structure with stacked pads, and obtained a milliamper level current from one single pad structure. The high current attributes to not only the large emission areas around the pad edge but also the excellent field emission performance of GaN material [48].

In general, semiconductor materials, for example, silicon, are favorably compatible with IC technology but encounter application problems in nanoscale vacuum devices due to their intrinsic shortcomings including an unstable chemical property, poor heat dissipation, and low conductivity, etc. [69] Therefore, the conventional semiconductors gradually move toward wide bandgap semiconductors, such as SiC and GaN [70]. In fact, the nanoscale vacuum devices employing SiC or GaN can endure more harsh environmental circumstances with high temperatures and strong radiation than their silicon competitors. Metal field emitters are also shown to be relatively insensitive to radiation damages or temperature changes under the onset of thermionic emission, mainly because of their undoped and amorphous properties. Unlike silicon, some new materials such as carbon nanotubes, graphene, and some kinds of nanowires, although having good field emission abilities as well as physical and chemical properties, also encounter application problems due to the poor compatibility with the microfabrication process.

4. Conclusions

The nanoscale vacuum devices fabricated by silicon-based process lines not only have many properties similar to solid-state devices such as small size, light weight, high integration, high efficiency, and no preheating time but also hold the ballistic electron transmission characteristic of traditional vacuum tubes. The comprehensive superiorities of the devices have attracted more attention from many research institutions since their invention, and research on device principles, materials, and processes has been carried out in the recent decade. Many new device designs including lateral structure, vertical structure, and gate-all-around structure are proposed and realized, and hopeful electric properties are obtained. Besides traditional semiconductor materials for solid-state IC and low work function refractory metals for field emission cathodes, the third-generation wide bandgap semiconductor materials, represented by SiC and GaN, and some new nanomaterials including carbon nanotubes, graphene, and some kinds of nanowires are also employed in the nanoscale vacuum devices to improve the device performance.

The solid-state devices or ICs are still unrivaled in most normal applications because of their well-developed technologies. However, the nanoscale vacuum devices are expected to make breakthroughs in some special areas such as high-temperature or strong radiation application environments. High-temperature industrial applications include electric vehicles, electric aircraft, space exploration, and deep-earth oil/gas extraction [71], where the high temperature always results in internal junction deterioration or leakage increase of traditional solid-state devices. The most typical radiation application is deep space exploration [7], where the accumulation of space radiation particles can damage nanoscale

solid-state electron devices, resulting in the decrease of on-state current, the increase of leakage current, the logic confusion of circuits, etc., and some catastrophic damages of them even cannot be dealt with by system backup.

Author Contributions: Conceptualization, X.L. and J.F.; writing—original draft preparation, X.L.; writing—review and editing, J.F. All authors have read and agreed to the published version of the manuscript.

Funding: This research was funded by the National Natural Science Foundation of China, Grant No. 61831001.

Data Availability Statement: Data sharing not applicable.

Conflicts of Interest: The authors declare no conflict of interest.

References

1. Brinkman, W.F.; Haggan, D.E.; Troutman, W.W. A history of the invention of the transistor and where it will lead us. *IEEE J. Solid-State Circuits* **1997**, *32*, 1858–1865. [[CrossRef](#)]
2. Barbour, E. The cool sound of tubes. *IEEE Spectrum* **1998**, *35*, 24–35. [[CrossRef](#)]
3. Symons, R.S. Tubes: Still Vital After All These Years. *IEEE Spectrum* **1998**, *35*, 52–63. [[CrossRef](#)]
4. Gilmour, A.S.; Ebrary, I. *Klystrons, Traveling Wave Tubes, Magnetrons, Crossed-Field Amplifiers, and Gyrotrons*; Artech House: Norwood, MA, USA, 2011.
5. Armstrong, C.M.; Kowalczyk, R.; Zubyk, A.; Berg, K.; Meadows, C.; Chan, D.; Schoemehl, T.; Duggal, R.; Hinch, N.; True, R.B.; et al. A compact extremely high frequency MPM power amplifier. *IEEE Trans. Electron Devices* **2018**, *65*, 2183–2188. [[CrossRef](#)]
6. Pan, P.; Tang, Y.; Bian, X.; Zhang, L.; Lu, Q.; Li, Y.; Feng, Y.; Feng, J. A G-Band Traveling Wave Tube With 20 W Continuous Wave Output Power. *IEEE Electron Device Lett.* **2020**, *41*, 1833–1836. [[CrossRef](#)]
7. Kim, H.K. Vacuum transistors for space travel. *Nat. Electron.* **2019**, *2*, 374–375. [[CrossRef](#)]
8. Shoulders, K.R. Microelectronics Using Electron-Beam-Activated Machining Techniques. *Adv. Comput.* **1961**, *2*, 135–138. [[CrossRef](#)]
9. Spindt, C.A. A Thin-Film Field-Emission Cathode. *J. Appl. Phys.* **1968**, *39*, 3504–3505. [[CrossRef](#)]
10. Spindt, C.A.; Brodie, I.; Hunphrey, L. Physical Properties of Thin Film Field Emission Cathode with Molybdenum Cones. *J. Appl. Phys.* **1976**, *47*, 5248–5263. [[CrossRef](#)]
11. Gray, H.F.; Campisi, G.J.; Greene, R.F. A vacuum field effect transistor using silicon field emitter arrays. In Proceedings of the 1986 International Electron Devices Meeting (IEDM), Washington, DC, USA, 7–10 December 1986; pp. 776–777.
12. Park, S.S.; Park, D.I.; Hahm, S.H.; Lee, J.H.; Choi, H.C.; Lee, J.H. Fabrication of a Lateral Field Emission Triode with a High Current Density and High Transconductance Using the Local Oxidation of the Polysilicon Layer. *IEEE Trans. Electron Devices* **1999**, *46*, 1283–1289. [[CrossRef](#)]
13. Driskill-Smith, A.A.G.; Hasko, D.G.; Ahmed, H. Nanoscale field emission structures for ultra-low voltage operation at atmospheric pressure. *Appl. Phys. Lett.* **1997**, *71*, 3159–3161. [[CrossRef](#)]
14. Han, J.W.; Oh, J.S.; Meyyappan, M. Vacuum nanoelectronics: Back to the future?—Gate insulated nanoscale vacuum channel transistor. *Appl. Phys. Lett.* **2012**, *100*, 213505. [[CrossRef](#)]
15. Srisonphan, S.; Jung, Y.; Kim, H. Metal–oxide–semiconductor field-effect transistor with a vacuum channel. *Nat. Nanotech* **2012**, *7*, 504–508. [[CrossRef](#)] [[PubMed](#)]
16. Stoner, B.R.; Glass, J.T. Nothing is like a vacuum. *Nat. Nanotechnol.* **2012**, *7*, 485–487. [[CrossRef](#)] [[PubMed](#)]
17. America Institute of Physics. Return of the Vacuum Tube. Science Daily. 18 May 2012. Available online: <https://news.sciencemag.org/physics/2012/05/return-vacuum-tube> (accessed on 10 February 2020).
18. Feng, J.; Li, X.; Hu, J.; Cai, J. General Vacuum Electronics. *J. Electromagn. Eng. Sci.* **2020**, *20*, 1–8. [[CrossRef](#)]
19. Chang, W.T.; Hsu, H.J.; Pao, P.H. Vertical Field Emission Air-Channel Diodes and Transistors. *Micromachines* **2019**, *10*, 858. [[CrossRef](#)]
20. Higuchi, T.; Maisenbacher, L.; Liehl, A.; Dombi, P.; Hommelhoff, P. A nanoscale vacuum-tube diode triggered by few-cycle laser pulses. *Appl. Phys. Lett.* **2015**, *106*, 051109. [[CrossRef](#)]
21. Jones, W.M.; Lukin, D.; Scherer, A. Ultra-low turn-on field emission devices characterized at atmospheric pressures and high temperatures. In Proceedings of the 2016 International Vacuum Nanoelectronics Conference (IVNC), Vancouver, BC, Canada, 11–15 July 2016. [[CrossRef](#)]
22. Chang, W.T.; Chuang, T.Y.; Su, C.W. Metal-based asymmetric field emission diodes operated in the air. *Microelectron. Eng.* **2020**, *232*, 111418. [[CrossRef](#)]
23. Chang, W.T.; Cheng, M.C.; Chuang, T.Y.; Tsai, M.Y. Field Emission Air-Channel Devices as a Voltage Adder. *Nanomaterials* **2020**, *10*, 2378. [[CrossRef](#)]
24. Liu, M.; Fu, W.; Yang, Y.; Li, T.; Wang, Y. Excellent field emission properties of VO₂(A) nanogap emitters in air. *Appl. Phys. Lett.* **2018**, *112*, 093104. [[CrossRef](#)]

25. Sapkota, K.R.; Leonard, F.; Talin, A.A.; Gunning, B.P.; Kazanowska, B.A.; Jones, K.S.; Wang, G.T. Ultralow Voltage GaN Vacuum Nanodiodes in Air. *Nano Lett.* **2021**, *21*, 1928–1934. [[CrossRef](#)]
26. Subramanian, K.; Kang, W.P.; Davidson, J.L. Nanocrystalline diamond lateral vacuum microtriode. *Appl. Phys. Lett.* **2008**, *93*, 203511. [[CrossRef](#)]
27. Subramanian, K.; Kang, W.P.; Davidson, J.L.; Ghosh, N.; Galloway, K.F. A review of recent results on diamond vacuum lateral field emission device operation in radiation environments. *Microelectron. Eng.* **2011**, *88*, 2924–2929. [[CrossRef](#)]
28. Pescini, L.L.; Tilke, A.; Blick, R.H.; Lorenz, H.; Kotthaus, J.P.; Eberhardt, W.; Kern, D. Nanoscale lateral field-emission triode operating at atmospheric pressure. *Adv. Mater.* **2001**, *13*, 1780–1783. [[CrossRef](#)]
29. Chang, W.T.; Pao, P.H. Field Electrons Intercepted by Coplanar Gates in Nanoscale Air Channel. *IEEE Trans. Electron Devices* **2019**, *66*, 3961–3966. [[CrossRef](#)]
30. Kim, J.; Kim, J.; Oh, H.; Meyyappan, M.; Han, J.W.; Lee, J.S. Design guidelines for nanoscale vacuum field emission transistors. *J. Vac. Sci. Technol. B* **2016**, *34*, 042201. [[CrossRef](#)]
31. Han, J.W.; Meyyappan, M. The device made of nothing. *IEEE Spectrum* **2014**, *51*, 30–35. [[CrossRef](#)]
32. Han, J.W.; Oh, J.S.; Meyyappan, M. Cofabrication of vacuum field emission transistor (VFET) and MOSFET. *IEEE Trans. Nanotechnol.* **2014**, *13*, 464–468. [[CrossRef](#)]
33. Xu, J.; Wang, Q.; Tao, Z.; Zhai, Y.; Chen, G.; Qi, Z.; Zhang, X. High-Quality and Stable Electron Emission Device with Sub-30-nm Aligned Nanogap Arrays. *IEEE Trans. Electron Devices* **2017**, *64*, 2364–2368. [[CrossRef](#)]
34. Nirantar, S.; Ahmed, T.; Ren, G.; Gutruf, P.; Xu, C.; Bhaskaran, M.; Walia, S.; Sriram, S. Metal–Air Transistors: Semiconductor-free field-emission air-channel nanoelectronics. *Nano Lett.* **2018**, *18*, 7478–7484. [[CrossRef](#)]
35. Spindt, C.A.; Holland, C.E.; Rosengreen, A.; Brodie, I. Field-emitter arrays for vacuum microelectronics. *IEEE Trans. Electron Devices* **1991**, *38*, 2355–2363. [[CrossRef](#)]
36. Hirano, T.; Kanemaru, S.; Tanoue, H.; Itoh, J. Fabrication of a New Si Field Emitter Tip with Metal-Oxide-Semiconductor Field-Effect Transistor (MOSFET) Structure. *Jpn. J. Appl. Phys.* **1996**, *35*, 6637–6640. [[CrossRef](#)]
37. Bozler, C.O.; Harris, C.T.; Rabe, S.; Rathman, D.D.; Smith, H.I. Arrays of gated field-emitter cones having 0.32 μm tip-to-tip spacing. *J. Vac. Sci. Technol. B* **1994**, *12*, 629–632. [[CrossRef](#)]
38. Park, I.J.; Jeon, S.G.; Shin, C. A New Slit-Type Vacuum-Channel Transistor. *IEEE Trans. Electron Devices* **2014**, *61*, 4186–4191. [[CrossRef](#)]
39. Shen, Z.; Wang, X.; Wu, S.L.; Tian, J. A new kind of vertically aligned field emission transistor with a cylindrical vacuum channel. *Vacuum* **2017**, *137*, 163–168. [[CrossRef](#)]
40. Han, J.W.; Seol, M.L.; Moon, D.I.; Hunter, G.; Meyyappan, M. Nanoscale vacuum channel transistors fabricated on silicon carbide wafers. *Nat. Electron.* **2019**, *2*, 405–411. [[CrossRef](#)]
41. Leobandung, E.; Gu, J.; Guo, L.; Chou, S.Y. Wire-channel and wrap-around-gate metal-oxide-semiconductor field-effect transistors with a significant reduction of short channel effects. *J. Vac. Sci. Technol. B* **1997**, *15*, 2791–2794. [[CrossRef](#)]
42. Colinge, J.P.; Gao, M.H.; Romano, A.; Maes, H.; Claeys, C. Silicon-on-insulator “gate-all-around” MOS device. In Proceedings of the 1990 IEEE SOS/SOI Technology Conference, Key West, FL, USA, 2–4 October 1990; pp. 137–138. [[CrossRef](#)]
43. Singh, N.; Agarwal, A.; Bera, L.K.; Liow, T.Y.; Yang, R.; Rustagi, S.C.; Tung, C.H.; Kumar, R.; Lo, G.Q.; Balasubramanian, N.; et al. High-performance fully depleted silicon nanowire (diameter ≤ 5 nm) gate-all-around CMOS devices. *IEEE Electron Device Lett.* **2006**, *27*, 383–385. [[CrossRef](#)]
44. Han, J.W.; Ahn, J.H.; Choi, Y.K. Damage immune field effect transistors with vacuum gate dielectric. *J. Vac. Sci. Technol. B* **2011**, *29*, 011014. [[CrossRef](#)]
45. Han, J.W.; Moon, D.I.; Oh, J.S.; Choi, Y.K.; Meyyappan, M. Vacuum gate dielectric gate-all-around nanowire for hot carrier injection and bias temperature instability free transistor. *Appl. Phys. Lett.* **2014**, *104*, 253506. [[CrossRef](#)]
46. Han, J.W.; Moon, D.I.; Meyyappan, M. Nanoscale Vacuum Channel Transistor. *Nano Lett.* **2017**, *17*, 2146–2151. [[CrossRef](#)] [[PubMed](#)]
47. Liu, M.; Liang, S.; Shi, D.; Yang, S.; Lei, Y.; Li, T.; Wang, Y. An emission stable vertical air channel diode by a low-cost and IC compatible BOE etching process. *Nanoscale* **2021**, *13*, 5693–5699. [[CrossRef](#)] [[PubMed](#)]
48. Wei, Y.; Zhao, H.; Zhao, J.; Huang, R.; Wang, J.; Chen, F.; Zhang, J.; Li, M. GaN Nanoscale Air Channel Devices with mA-level Output by IC compatible processes. In Proceedings of the 2022 International Vacuum Nanoelectronics Conference (IVNC), Seoul, Republic of Korea, 5–8 July 2022; pp. 17–18.
49. Han, J.W.; Seol, M.L.; Meyyappan, M. A nanoscale vacuum field emission gated diode with an umbrella cathode. *Nanoscale Adv.* **2021**, *3*, 1725–1729. [[CrossRef](#)] [[PubMed](#)]
50. Lenk, C.; Lenk, S.; Holz, M.; Guliyev, E.; Hofmann, M.; Ivanov, T.; Rangelow, I.W.; Behzadirad, M.; Rishinaramangalam, A.K.; Feezell, D.; et al. Experimental study of field emission from ultrasharp silicon, diamond, GaN, and tungsten tips in close proximity to the counter electrode. *J. Vac. Sci. Technol. B* **2018**, *36*, 06JL03. [[CrossRef](#)]
51. Bhattacharya, R.; Turchetti, M.; Keathley, P.D.; Berggren, K.K.; Browning, A. Long term field emission current stability characterization of planar field emitter devices. *J. Vac. Sci. Technol. B* **2021**, *39*, 053201. [[CrossRef](#)]
52. Li, X.; Han, P.; Xie, Y.; Du, T.; Cai, J.; Feng, J. Environments adaptability and failure analysis of nanoscale vacuum channel transistors. In Proceedings of the 2020 IEEE International Conference on Vacuum Electronics (IVEC), Monterey, CA, USA, 20–23 April 2020; pp. 381–382.

53. Rose, L.B.D.; Scherer, A.; Jones, W.M. Suspended Nanoscale Field Emitter Devices for High-Temperature Operation. *IEEE Trans. Electron Devices* **2020**, *67*, 5125–5131. [[CrossRef](#)]
54. Novoselov, K.S.; Geim, A.K.; Morozov, S.V.; Jiang, D.; Zhang, Y.; Dubonos, S.V.; Grigorieva, I.V.; Firsov, A.A. Electric Field Effect in Atomically Thin Carbon Films. *Science* **2004**, *306*, 666–669. [[CrossRef](#)]
55. Castro Neto, A.H.; Guinea, F.; Peres, N.M.R.; Novoselov, K.S.; Geim, A.K. The electronic properties of graphene. *Rev. Mod. Phys.* **2009**, *81*, 109–162. [[CrossRef](#)]
56. Marconcini, P.; Macucci, M. The k.p method and its application to graphene, carbon nanotubes and graphene nanoribbons: The Dirac equation. *Riv. Nuovo Cim.* **2011**, *34*, 489–584. [[CrossRef](#)]
57. Giannazzo, F.; Greco, G.; Roccaforte, F.; Sonde, S.S. Vertical Transistors Based on 2D Materials: Status and Prospects. *Crystals* **2018**, *8*, 70. [[CrossRef](#)]
58. Chavarin, C.A.; Strobel, C.; Kitzmann, J.; Bartolomeo, A.D.; Lukosius, M.; Albert, M.; Bartha, J.W.; Wenger, C. Current Modulation of a Heterojunction Structure by an Ultra-Thin Graphene Base Electrode. *Materials* **2018**, *11*, 345. [[CrossRef](#)] [[PubMed](#)]
59. Wu, G.; Wei, X.; Zhang, Z.; Chen, Q.; Peng, L. A Graphene-Based Vacuum Transistor with a High ON/OFF Current Ratio. *Adv. Funct. Mater.* **2015**, *25*, 5972–5978. [[CrossRef](#)]
60. Xu, J.; Gu, Z.; Yang, W.; Wang, Q.; Zhang, X. Graphene-Based Nanoscale Vacuum Channel Transistor. *Nanoscale Res. Lett.* **2018**, *13*, 311. [[CrossRef](#)] [[PubMed](#)]
61. Neudeck, P.; Krasowski, M.; Prokop, N. Assessment of durable SiC JFET technology for +600 °C to –125 °C integrated circuit operation. *ECS Trans.* **2011**, *8*, 163–176. [[CrossRef](#)]
62. Wang, L.; Wei, G.; Gao, F.; Li, C.; Yang, W. High-temperature stable field emission of b-doped SiC nanoneedle arrays. *Nanoscale* **2015**, *7*, 7585–7592. [[CrossRef](#)]
63. Liu, M.; Li, T.; Wang, Y. SiC emitters for nanoscale vacuum electronics: A systematic study of cathode–anode gap by focused ion beam etching. *J. Vac. Sci. Technol. B* **2017**, *35*, 031801. [[CrossRef](#)]
64. Kozawa, T.; Suzuki, M.; Taga, Y.; Gotoh, Y.; Ishikawa, J. Fabrication of GaN field emitter arrays by elective area growth technique. *J. Vac. Sci. Technol. B* **1998**, *16*, 833–835. [[CrossRef](#)]
65. Ławrowski, R.; Langer, C.; Prommesberger, C.; Schreiner, R. Microrods and microlines by three-dimensional epitaxially grown GaN for field emission cathodes. In Proceedings of the 2017 International Vacuum Nanoelectronics Conference (IVNC), Regensburg, Germany, 10–14 July 2017; pp. 130–131.
66. Pearton, S.J.; Ren, F.; Patrick, E.; Law, M.E.; Alexander, Y. Polyakov. Review-Ionizing Radiation Damage Effects on GaN Devices. *ECS J. Solid State Sci. Technol.* **2016**, *5*, Q35–Q60. [[CrossRef](#)]
67. Zhao, D.S.; Liu, R.; Fu, K.; Yu, G.; Cai, Y.; Huang, H.; Wang, Y.; Sun, R.; Zhang, B. An Al_{0.25}Ga_{0.75}N/GaN Lateral Field Emission Device with a Nano Void Channel. *Chin. Phys. Lett.* **2018**, *35*, 114–117. [[CrossRef](#)]
68. Wang, G.T.; Sapkota, K.R.; Talin, A.A.; Leonard, F.; Gunning, B.P.; Vizelethy, G. Ultra-low Voltage GaN Vacuum Nanoelectronics. In Proceedings of the 2022 Compound Semiconductor Week (CSW), Ann Arbor, MI, USA, 1–3 June 2022; pp. 1–2.
69. Sze, S.M.; Ng, K.K. *Physics and Properties of Semiconductors—A Review in Physics of Semiconductor Devices*; Wiley: Hoboken, NJ, USA, 2006; pp. 5–75.
70. Neudeck, P.G.; Okojie, R.S.; Chen, L.Y. High-temperature electronics—A role for wide bandgap semiconductors? *Proc. IEEE* **2002**, *90*, 1065–1076. [[CrossRef](#)]
71. Guo, X.; Xun, Q.; Li, Z.; Du, S. Silicon carbide converters and MEMS devices for high-temperature power electronics: A critical review. *Micromachines* **2019**, *10*, 406. [[CrossRef](#)] [[PubMed](#)]

Disclaimer/Publisher’s Note: The statements, opinions and data contained in all publications are solely those of the individual author(s) and contributor(s) and not of MDPI and/or the editor(s). MDPI and/or the editor(s) disclaim responsibility for any injury to people or property resulting from any ideas, methods, instructions or products referred to in the content.